problem. Therefore, the use of MT signals and spectral averaging before estimation is required to maintain acceptable performances when operating near or below the indicated threshold.

The validation of the present analysis on real underwater data and the extension of the analysis to echo processors operating in the time domain is under investigation by the authors.

References

[1] K. B. Theriault, "Incoherent multibeam Doppler current profiler performance: Part I—Estimate variance," *IEEE J. Ocean. Eng.*, vol. OE-11, no. 1, pp. 7–15, Jan. 1986.

[2] F. Andreucci, C. Camporeale, and F. Fogliuzzi, "Acoustic wideband techniques for the remote estimation of the sea current velocity," in *Proc. European Conf. Underwater Acoustics*, Luxembourg, Sept. 1992, pp. 729–732.

[3] R. Pinkel, M. Merrifield, G. Deane, and J. Smith, "Doppler acoustic studies of fine scale variability in the Arctic Ocean," in *Proc. European Conf. Underwater Acoustics*, Luxembourg, Sept. 1992, pp. 17–23.

[4] F. Andreucci, C. Camporeale, and F. Fogliuzzi, "Acoustic wideband techniques for the remote estimation of the sea current velocity," in *OCEANS'92 Conf. Proc.*, Newport, RI, Oct. 1992, pp. 614–619.

[5] A. Papoulis, *Signal Analysis*. New York: McGraw-Hill, 1977.

[6] A. Papoulis, *Probability, Random Variables, and Stochastic Processes*, 2nd ed. New York: McGraw-Hill, 1986.

An Efficient Architecture for Real-Time Narrowband Beamforming

Yan W. Zhang and Yuan L. Ma

Abstract—**A short finite impulse response (FIR) filter architecture for narrowband beamforming is presented that is well suited for active sonar applications. By applying the technique of adaptive modeling, a short FIR filter can be designed to carry out any required narrowband constant phase shift. A 4-tap FIR filter designed in this way can generate constant phase shift within bandwidths of 0.04 (relative to the sampling frequency), with an error of less than 1°. Thus a beam can be formed with a bank of short FIR filters, each filter corresponding to one sensor. Due to the light computational load of this method, it is rather convenient for digital signal processors (DSP) to implement beamforming in real time. Satisfactory sonar beampatterns are shown to result from a TMS320C25-based emulation of the architecture.**

I. Introduction

The use of time-delay-sum beamforming in underwater acoustic signal processing typically relies on the use of a high sampling rate or time-domain interpolation [1] to form a large number of synchronous beams. For the narrowband case, phase shift is often implemented instead of time delay, in order to take advantage of the narrowband phase structure. In this way, beamforming involves no more processing than narrowband phase shift, amplitude weighting, and summation. There is no problem with the implementation of amplitude weighting and summation. The crux lies in how narrowband phase shift can be conveniently obtained.

Manuscript received January 15, 1993; revised April 1, 1994.

The authors are with the College of Marine Engineering, Northwestern Polytechnical University, Xi'an 710072, Shaanxi Province, People's Republic of China.

IEEE Log Number 9405274.

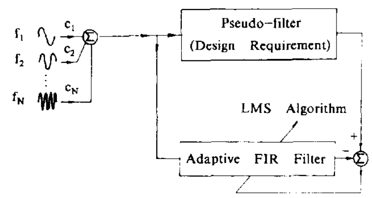

Fig. 1. Phase shifter design employing adaptive modeling.

With the conventional method of quadrature beamforming [2], two local oscillating signals, two multipliers and two low-pass filters are needed for each sensor. This is an inconvenient architecture for practical use. This may be improved with a simplified approach [3] where the -90° phase shift for the quadrature component is accomplished by a time delay of $1/4f_0$ (f_0 being the central frequency of the narrowband signal). However, in general, quadrature beamformers are affected by high rates of Doppler frequency shift. For instance, at $f_0 = 4$ kHz a Doppler range of ± 170 Hz will result in phase errors of up to $\pm 3.8^\circ$. This may cause an unsatisfactory beam pattern.

The communication presents a novel approach for generating any required narrowband constant phase shift. The approach employs an FIR filter with only 4 or 5 taps. Beam patterns generated with this approach are shown to be satisfactory and more robust to Doppler frequency shifts than the quadrature beamformer. The light computational load of the short FIR filter results in a beamformer architecture that is well suited for real-time application. This is demonstrated with a TMS320C25 hardware implementation of the beamformer.

II. Design Principles

The technique of adaptive modeling [4], [5] is applied. As shown in Fig. 1, a signal source composed of N sinusoids corresponding to N design frequencies serves as the input of both a pseudofilter (depicting the design requirement) and an adaptive FIR filter. The composition of signal source is shown as follows:

$$x(n) = \sum_{i=1}^{N} c_i \cos(2\pi f_i n). \tag{1}$$

The output of the pseudofilter, i.e., the expected output of the adaptive filter is

$$d(n) = \sum_{i=1}^{N} c_i \cos(2\pi f_i n + \varphi) \tag{2}$$

where φ is the desired phase shift and c_i is a positive cost factor for frequency f_i. The larger c_i is, the more tightly will the specification be held at frequency f_i.

The LMS algorithm is employed to adjust the adaptive FIR filter. After the adaptive filter converges, a set of stable-state coefficients is obtained. An FIR filter with these coefficients as its impulse response can implement the narrowband constant phase shift specified by the pseudofilter.

Consider the design of such a beamformer at the central frequency = 0.2 (all frequencies are normalized by the sampling frequency). It is required that within the band of 0.18–0.22, a phase shifter be designed to implement a -90° phase shift and that the

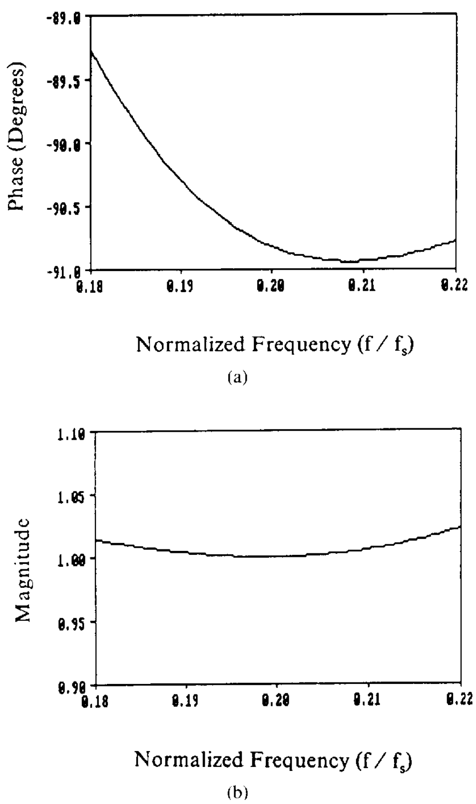

Fig. 2. Frequency response of the designed $-90°$ phase shifter. (a) Phase. (b) Magnitude.

magnitude response over the band be undistorted. In the design, the FIR filter is set to be 4-tap. The input signal source is parameterized such that $f_1 = 0.15$, $f_2 = 0.175$, $f_3 = 0.2$, $f_4 = 0.225$, $f_5 = 0.25$, $c_1 = 1$, $c_2 = 1.8$, $c_3 = 1.8$, $c_4 = 1.8$, and $c_5 = 1$ (referring to (1)). The transfer function of the obtained 4-tap filter is as follows:

$$H(z) = -0.4971209 + 1.684239z^{-1} - 0.4887393z^{-2} + 0.5352885z^{-3}. \quad (3)$$

Its output phase and magnitude response versus frequency is shown in Fig. 2 (a) and (b). Within the band, the phase response is close to $-90°$ with a maximum error of less than $1°$; the magnitude response at the central frequency is 1 and is relatively flat within the band, deviating only by $(MAG_{max} - MAG_{min})/MAG_{min} = 2.27\%$. These approximately satisfy the design requirements. Note that similar FIR filters have been successfully designed for other frequency regions.

The impulse response of a similar length FIR filter implementing an arbitrary phase shift φ can be simply deduced if the parameters for the $-90°$ phase shift filter are known. Suppose the transfer function of a 4-tap FIR filter implementing a $-90°$ phase shift is

$$K(z) = k_0 + k_1z^{-1} + k_2z^{-2} + k_3z^{-3}. \quad (4)$$

Denote the input narrowband signal as

$$x(n) = A(n)\cos[2\pi f_0 n + \Psi(n)]$$

where $A(n)\exp[j\Psi(n)]$ is the baseband complex envelope of $x(n)$.

If the desired phase shift is φ, the required output should be

$$\begin{aligned} A(n)&\cos[2\pi f_0 n + \Psi(n) + \varphi] \\ &= A(n)\cos[2\pi f_0 n + \Psi(n)]\cos\varphi \\ &\quad - A(n)\sin[2\pi f_0 n + \Psi(n)]\sin\varphi \\ &= x(n)\cos\varphi - \hat{x}(n)\sin\varphi \end{aligned} \quad (5)$$

where $\hat{\boldsymbol{x}}(n)$ denotes the Hilbert transform of $x(n)$. According to (4), with $x(n)$ as input, the output of the $K(z)$ filter is just the Hilbert transform of $x(n)$, i.e.,

$$\hat{\boldsymbol{x}}(n) = x(n)k_0 + x(n-1)k_1 + x(n-2)k_2 + x(n-3)k_3. \quad (6)$$

Combining (5) and (6), the required output with phase shift φ is

$$\begin{aligned} A(n)&\cos[2\pi f_0 n + \Psi(n) + \varphi] \\ &= x(n)\cos\varphi - \sin\varphi[x(n)k_0 + x(n-1)k_1 \\ &\quad + x(n-2)k_2 + x(n-3)k_3] \\ &= [\cos\varphi - \sin\varphi k_0]x(n) - \sin\varphi k_1 x(n-1) \\ &\quad - \sin\varphi k_2 x(n-2) - \sin\varphi k_3 x(n-3). \end{aligned} \quad (7)$$

Thus the four coefficients of the 4-tap FIR filter implementing phase shift φ are

$$\begin{aligned} a_0 &= \cos\varphi - \sin\varphi k_0 \\ a_1 &= -\sin\varphi k_1 \\ a_2 &= -\sin\varphi k_2 \\ a_3 &= -\sin\varphi k_3. \end{aligned}$$

The corresponding transfer function will be

$$A(z) = a_0 + a_1z^{-1} + a_2z^{-2} + a_3z^{-3}.$$

For example, within the normalized band of 0.18–0.22, a $23°$ phase shift is required. Based on the $-90°$ phase-shift FIR filter specified by (3), the transfer function of the $23°$ phase-shift FIR filter can be deduced to be

$$A(z) = 1.114745 - 0.6580846z^{-1} + 0.1909657z^{-2} - 0.2091539z^{-3}.$$

Although the arbitrary phase-shift filters, derived from the $-90°$ filter, also have an implicit phase and magnitude distortion error over the band, these errors are shown to be maximum for $\varphi = -90°$ (see Appendix).

The above principle is illustrated in Fig. 3. Therefore, as long as the $-90°$ phase-shift filter is obtained, arbitrary phase-shift filters can be deduced conveniently. This is favorable for practical beamforming applications, where multiple beams may be required. Given the normalized bandwidth of 0.04, the robustness of proposed short FIR beamformer to Doppler frequency shift may be illustrated. Consider a linear FM signal that is transmitted from an active sonar. The assumed central frequency is 4 kHz, and the sweep extent is 200 Hz. The sampling frequency is set to be 15 kHz. Suppose a target is moving within a speed range of ± 60 knots. Then the maximum Doppler frequency shift will be less than ± 170 Hz (assuming the underwater sound speed to be 1500 m/s), i.e., the maximum Doppler bandwidth will be 340 Hz. The overall bandwidth will be 540 Hz (= 200 + 340). Expressed as normalized frequency (relative to the sampling frequency), this bandwidth is 0.036, which is smaller than 0.04. Hence, this technique improves on the Doppler robustness of the beamformer.

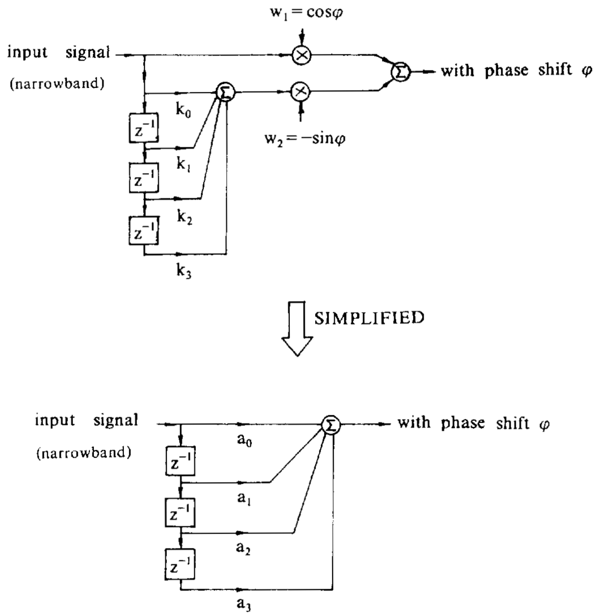

Fig. 3. Generation of narrowband arbitrary phase shift filter.

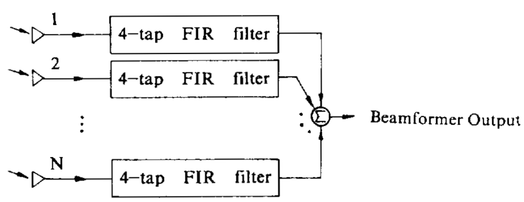

Fig. 4. Short FIR filter architecture of the narrowband beamformer.

III. Real-Time Hardware Implementation of the Short FIR Architecture

Based on the method presented above, an efficient architecture for narrowband beamforming may be realized. Because of the narrow operational band of the beamformer, it is ideally suited for active sonar applications. As illustrated in Fig. 4, the output of each sensor is appropriately phase shifted by its corresponding short FIR filter. The outputs of all sensor FIR filters are then summed up to provide the beam output. Amplitude weighting for each sensor is realized as a multiplying factor applied to the sensor's FIR filter coefficients.

The short FIR beamformer architecture shown in Fig. 4 is implemented with the use of two TMS320C25 processor chips [6]. In this emulation a 16-element line array is beamformed such that 16 beams are formed over 360° in the horizontal plane. The assumed sampling frequency is 12 kHz. Note that this array is baffled on one side.

For each beam, sixteen 4-tap FIR filters are put into use, one filter at each sensor. Hence there are 64 (= 4 × 16) filter coefficients for one beam, 1024 (= 64 × 16) filter coefficients for all the 16 beams. Notice that 1024 FIR filter coefficients are computed and then stored in the memory beforehand. The total computational load of multiple filtering to form 16 beams is 1024 multiply/adds.

To form 16 beams, the whole process of fetching sensor data, multiple filtering, and storing beam outputs takes 1600 TMS320C25 instruction cycles. This is equivalent to a processing time of 160 μs assuming a TMS320C25 (40MHz) instruction cycle of 100 ns. For the 12-kHz sampling frequency, the sampling interval is 83.3 μs. Hence two TMS320C25 working in parallel must be used to form the 16 beams in real time.

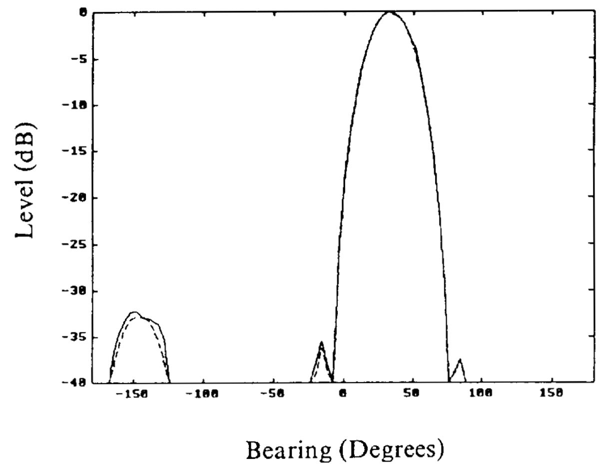

Fig. 5. Comparison between emulated (solid) and theoretical (dashed) beampatterns.

Fig. 5 is a computer-generated beam pattern (at one frequency within the small operational band) for a beam near 30° from forward endfire. It contains the abovementioned phase and magnitude distortion errors caused by the short FIR filters, together with finite word length effects from the use of 12-bit sensor data and 16-bit FIR filter coefficients. The theoretical beampattern with ideal phase and magnitude are shown with the dashed line. The two beampatterns show little difference. This is also the case with beam patterns generated for the other 15 beams and for other frequencies within the small operational band. Hence, the small errors introduced by the beamformer's short FIR filters can be tolerated.

IV. Conclusion

With a short FIR filter (4 or 5 tap), narrowband constant phase shift can be accomplished. The phase and magnitude distortion errors observed with the use of the short FIR filter for beamforming showed no significant degradation in the beamformer spatial response. Based on this technique, an efficient narrowband beamforming architecture can be realized. The short-FIR-filter architecture has a light computational load that can be easily carried out by commonly available DSP chips. A hardware implementation of the proposed beamformer with TMS320C25 processor chips demonstrates the real-time potential of this beam-forming architecture in active sonar applications.

V. Appendix

Analysis of Error Caused by the Phase Shift Filter

For any frequency f within the narrowband, suppose the designed $-90°$ phase-shift filter transforms $\cos(2\pi f n)$ into $A\sin(2\pi f n + \theta)$, where $A \neq 1$ and $\theta \neq 0°$ are the magnitude distortion error and the phase error, respectively.

According to the principle illustrated in Fig. 3, for any phase shift $\varphi \neq -90°$, the required FIR filter can be deduced from the $-90°$ phase shift filter.

For phase shift φ, the filter-generated output will be

$$y_1(n) = \cos(2\pi f n)\cos\varphi - A\sin(2\pi f n + \theta)\sin\varphi.$$

The ideal phase shift output is

$$y_2(n) = \cos(2\pi f n)\cos\varphi - \sin(2\pi f n)\sin\varphi.$$

The difference between $y_1(n)$ and $y_2(n)$ is

$$\begin{aligned} y_2(n) - y_1(n) &= A\sin(2\pi f n + \theta)\sin\varphi - \sin(2\pi f n)\sin\varphi \\ &= \sin\varphi[A\sin(2\pi f n + \theta) - \sin(2\pi f n)] \\ &= \sin\varphi[(A\cos\theta - 1)\sin(2\pi f n) \\ &\quad + A\sin\theta\cos(2\pi f n)] \\ &= \sin\varphi\sqrt{A^2 + 1 - 2A\cos\theta}\,\sin(2\pi f n + \beta) \end{aligned}$$

where

$$\beta = \mathrm{tg}^{-1}\frac{A\sin\theta}{A\cos\theta - 1}.$$

The amplitude of error is

$$D(\varphi) = |\sin\varphi|\sqrt{A^2 + 1 - 2A\cos\theta}.$$

Thus it is clear that when $\varphi = -90°$, the amplitude of error reaches its maximum.

ACKNOWLEDGMENT

The authors are grateful to the reviewers and editors for their helpful comments. We also wish to thank Y. Q. Du for her work in preparing the manuscript.

REFERENCES

[1] D. C. M. Horvat, J. S. Bird, and M. M. Goulding, "True time-delay bandpass beamforming," *IEEE J. Oceanic Eng.*, vol. 17, no. 2, pp. 185–192, Apr. 1992.

[2] R. O. Nielsen, *Sonar Signal Processing*. Norwood, MA: Artech House, 1991.

[3] O. D. Grace and S. P. Pitt, "Sampling and interpolation of bandlimited signals by quadrature methods," *J. Acoust. Soc. Amer.*, vol. 48, no. 6 (pt. 1), pp. 1311–1318, 1970.

[4] S. D. Stearns and R. A. David, *Signal Processing Algorithms*. Englewood Cliffs, NJ: Prentice-Hall, 1988.

[5] B. Widrow and S. D. Stearns, *Adaptive Signal Processing*. Englewood Cliffs, NJ: Prentice-Hall, 1985.

[6] Y. W. Zhang and Y. L. Ma, "A novel beamforming approach based on DSP chips," in *Proc. 14th Int. Congr. Acoustics*, vol. LP-7, Beijing, P. R. China, 1992.